The Astrophysical Journal Letters, 870:L7 (6pp), 2019 January 1 https://doi.org/10.3847/2041-8213/aaf8ac

Ultralow-amplitude RR Lyrae Stars in M4

Joshua J. Wallace, Joel D. Hartman, Gáspár Á. Bakos[1], and Waqas Bhatti
Department of Astrophysical Sciences, Princeton University, 4 Ivy Lane, Princeton, NJ 08544, USA; joshuajw@princeton.edu
Received 2018 November 1; revised 2018 December 13; accepted 2018 December 17; published 2019 January 3

Abstract

We report evidence for a new class of variable star, which we dub millimagnitude RR Lyrae (mmRR). From *K*2 observations of the globular cluster M4, we find that out of 24 horizontal branch stars not previously known to be RR Lyrae variables, two show photometric variability with periods and shapes consistent with those of first-overtone RR Lyrae variables. The variability of these two stars, however, has amplitudes of only one part in a thousand, which is ∼200 times smaller than for any RR Lyrae variable in the cluster, and much smaller than any known RR Lyrae variable generally. The periods and amplitudes are 0.33190704 day with 1.0 mmag amplitude, and 0.31673414 day with 0.3 mmag amplitude. The stars lie just outside the instability strip, one blueward and one redward. The star redward of the instability strip also exhibits significant multi-periodic variability at lower frequencies. We examine potential blend scenarios and argue that they are all either physically implausible or highly improbable. Stars such as these are likely to shed valuable light on many aspects of stellar physics, including the mechanism(s) that set amplitudes of RR Lyrae variables.

Key words: globular clusters: individual (M4) – stars: horizontal-branch – stars: individual (Gaia DR2 6045466571386703360, Gaia DR2 6045478558624847488) – stars: oscillations (including pulsations) – stars: peculiar (except chemically peculiar) – stars: variables: RR Lyrae

1. Introduction

RR Lyrae stars are valuable astronomical tools. They are used as standard candles and to measure the helium abundance of stars in globular clusters (GCs). Space-based monitoring of RR Lyrae variables by missions such as *Microvariability and Oscillations of Stars* (Walker et al. 2003), *CoRoT* (Baglin & COROT Team 1998), and *Kepler*/*K*2 (Howell et al. 2014) has revealed new information about these objects. For example, *Kepler* has revealed additional, low-amplitude oscillation modes in fundamental mode (RR0) RR Lyrae variables (Molnár et al. 2012), including RR Lyr itself (Benkő et al. 2010). See Molnár (2018) for a more complete list of these discoveries.

As part of continuing efforts to observe RR Lyrae stars, the GC M4 (NGC 6121) was observed by *Kepler*/*K*2 in 2014 during its Campaign 2 using a large superstamp that contained thousands of stars. This and other *K*2 observations of GCs are the longest continuous photometric surveys of populations of GC stars, monitored at the high precision that has been *Kepler*'s hallmark. As part of our analysis of these data, we have discovered two horizontal branch (HB) stars just outside the instability strip that have photometric variations similar to first-overtone RR Lyrae (RR1) pulsators, but with an amplitude that is ∼200 times lower than the typical lowest-amplitude RR1s. We tentatively give these stars the name "millimagnitude RR Lyrae," or "mmRR" for short. The two stars are *Gaia* DR2 6045466571386703360 (mmRR 1) and *Gaia* DR2 6045478558624847488 (mmRR 2). There is no previously identified variable class that matches the properties of these stars, and if their variability is associated with RR1 variability, then they would be by far the lowest-amplitude RR Lyrae variables yet discovered. Previous RR Lyrae searches would likely have been unable to find such low-amplitude objects, so it is not surprising that they are only now being discovered by *K*2.

[1] MTA Distinguished Guest Fellow, Konkoly Observatory.

2. Observations and Analysis

2.1. K2 Image Subtraction, Reduction, and Variable Search

Our light curve extraction pipeline is very similar to the image subtraction pipeline of Soares-Furtado et al. (2017). Our specific pipeline, briefly described here, will receive a full description in our publication of a catalog of M4 *K*2 variables. We downloaded the 16 target pixel files (*K*2 IDs 200004370–200004385) that make up the M4 superstamp from the Mikulski Archive for Space Telescopes (MAST) and stitched them together using `k2mosaic` (Barentsen 2016), producing a total of 3856 images. We removed images that were blank or that otherwise would produce low-quality photometry (usually due to excessive drift), and were left with 3724 images covering ∼78 days. We reduced these images to a set of registered, subtracted images using tools from the `FITSH` software package (Pál 2012).

We used the *Gaia* first data release (DR1) source catalog (Gaia Collaboration et al. 2016a, 2016b) as both an astrometric (Lindegren et al. 2016) and photometric (van Leeuwen et al. 2017) reference catalog. DR1 was used instead of the second data release (DR2) because our analysis began prior to DR2's release. A conversion between *Gaia* magnitude *G* and *Kepler* magnitude K_p was determined, which, owing to the similar bandpasses of the two telescopes, was purely linear. The converted *G* magnitudes were used as reference magnitudes for performing image subtraction photometry on the subtracted images, using `fiphot` from `FITSH` and a series of aperture sizes. The aperture used for a given magnitude was determined by calculating the rms scatter of the final light curves and finding the aperture that had the lowest median rms value in half-magnitude bins.

The light curves suffered from residual systematic variations due to the roll of the spacecraft. We performed a decorrelation

Table 1
Data on mmRRs

Gaia DR2 ID	*G* (mag)	R.A. (°)	decl. (°)	Period (day)	Amplitude (mmag)	Epoch (BJD-2454833.0)
6045466571386703360	13.212	245.88458510	−26.48151484	0.33190704	1.0	2059.57
6045478558624847488	13.047	245.89969745	−26.43914199	0.31673414	0.3	2059.47

Note. Magnitude and position information from *Gaia* DR2. Epoch is the time of maximum brightness.

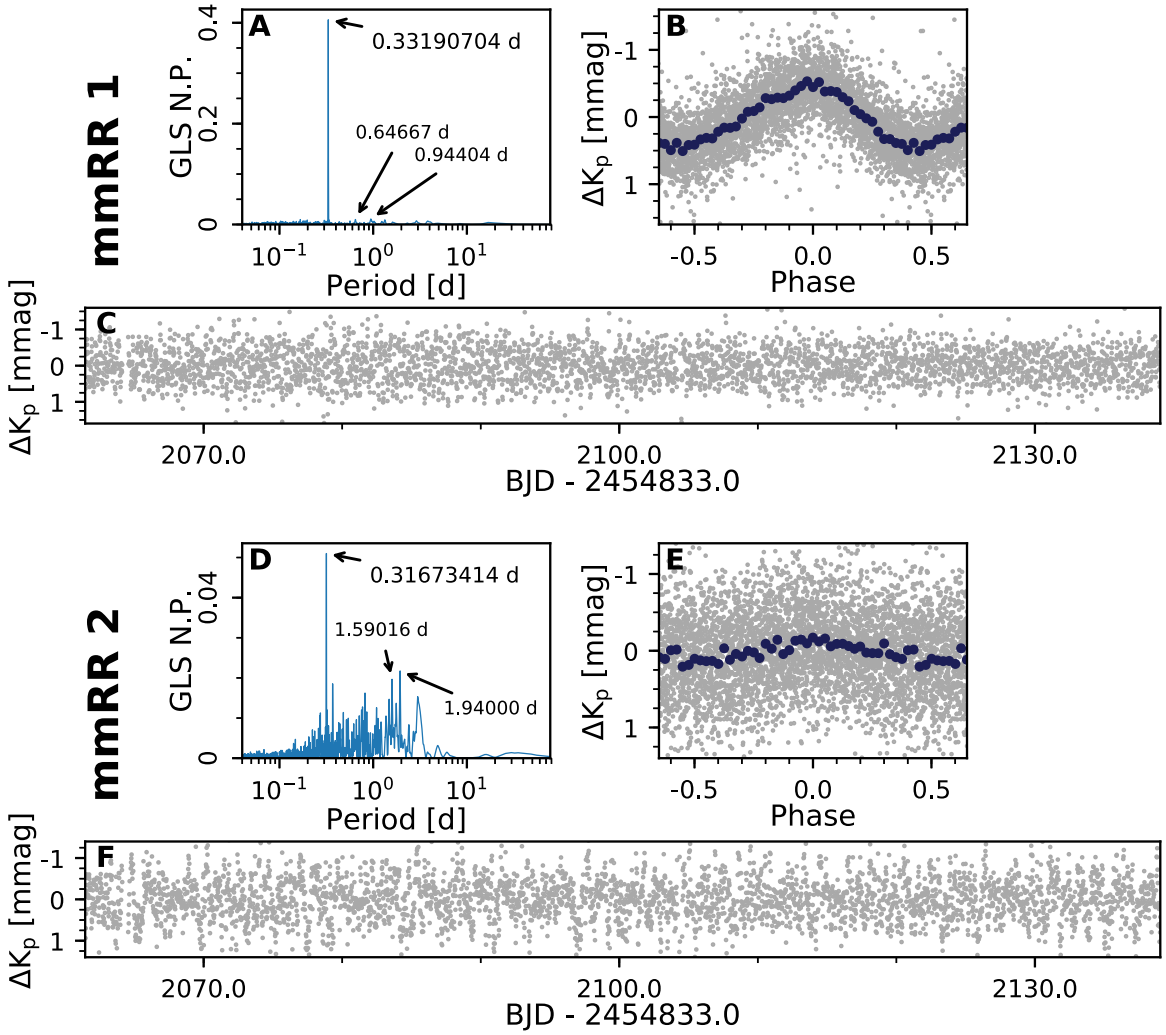

Figure 1. Light curves and periodograms for the two variable stars. Panels A, B, and C correspond to mmRR 1, and panels D, E, and F to mmRR 2. Panels A and D show the GLS normalized power (NP) spectra, with the three highest peaks in each case labeled. Panels B and E show the phased light curves of each star, each folded at the GLS period with the highest peak. Panels C and F show the full light curves for each star. Gray points show individual measurements, and blue points show binned-median values. All light curves have their median magnitudes subtracted off (mmRR 1: 13.14153, mmRR 2: 12.91269). We note possible notches in both phase-folded light curves just prior to maximum brightness.

of the measured photometry against the telescope roll using the process described by Vanderburg & Johnson (2014) and Vanderburg et al. (2016). As part of the decorrelation, a B-spline was also fit to the data with breakpoints set every 1.5 days and removed from the data. The `VARTOOLS` implementation (Hartman & Bakos 2016) of the trend-filtering algorithm (TFA; Kovács et al. 2005) was then used to further clean up global trends in the final photometry.

Light curves were obtained for 4600 *Gaia* DR1 sources, which were searched for variability using the Generalized Lomb–Scargle (GLS; Lomb 1976; Scargle 1982; Zechmeister & Kürster 2009), phase dispersion minimization (Stellingwerf 1978), box least squares (Kovács et al. 2002), and auto-correlation function (McQuillan et al. 2013) methods as implemented in `astrobase` (Bhatti et al. 2017). The results from these methods were searched by eye for significant variability.

2.2. The Horizontal Branch Stars

To determine cluster membership, we used *Gaia* DR2 proper motion measurements (Lindegren et al. 2018) to determine cluster membership. The proper motion of M4 ($\mu_{\alpha*} = -12.5$ mas yr^{-1}, $\mu_\delta = -19.0$ mas yr^{-1}) is well separated from that of the field population. We used `scikit-learn` (Pedregosa et al. 2011) to

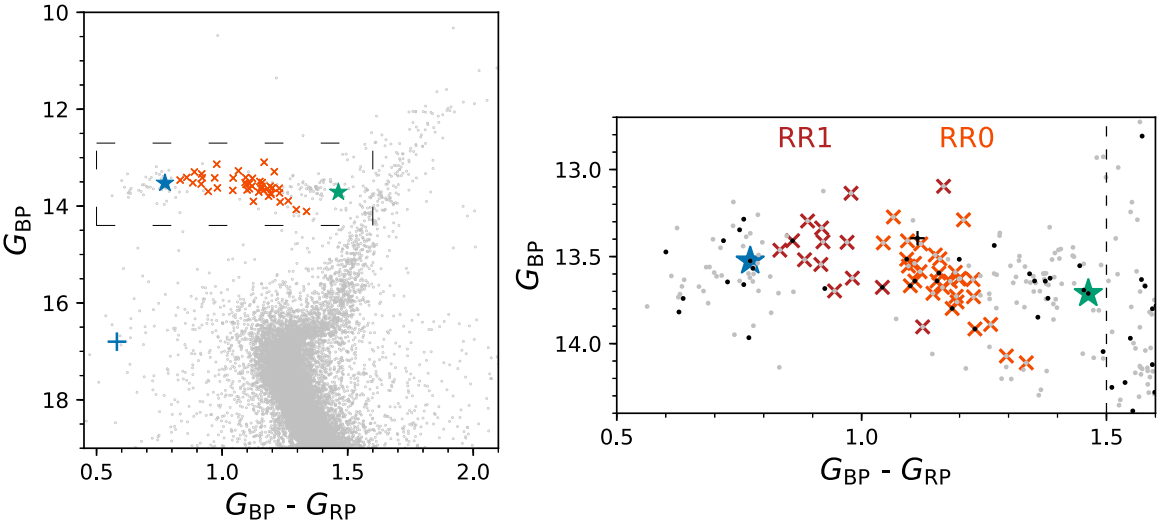

Figure 2. *Gaia* DR2 CMDs for M4, with G_{RP} and G_{BP} data taken from *Gaia* DR2 (Riello et al. 2018). Only objects with membership probabilities greater than 95% are included. Left panel: red x's mark stars previously identified as RR Lyrae in the catalog of Clement et al. (2001), 2016 June edition. The blue star marks mmRR 1, and the green star marks mmRR 2. The blue cross marks a particular star blended with mmRR 1 (Blend 1). Right panel: zoom-in of the portion of the left panel delineated by the dashed lines. RR Lyrae variables are differentiated by subclass: light red for RR0 and dark red for RR1, as indicated. For this panel, sources for which we have a *K*2 light curve are marked in black instead of gray. Star G3168 is marked with a black cross. Our $G_{BP} - G_{RP} < 1.5$ cut for investigated objects is shown with a vertical dashed line.

fit a two-component Gaussian mixture model to the proper motion measurements of all *Gaia* DR2 sources within 30′ of the cluster center with reported proper motions (for full details, see Wallace 2018).

This Letter presents results of a variability search among the 34 HB stars for which we had light curves. HB stars were selected to be those with $14.3 < G_{BP} < 13.0$ and $G_{BP} - G_{RP} < 1.5$ and a >95% cluster membership probability. Of these, 10 were previously identified as RR Lyrae variables (Clement et al. 2001). Of the other 24 HB stars, we identified two low-amplitude variables with $\lesssim$1 mmag amplitude sinusoidal variability and periods of ∼0.3 day and fell outside the locus of identified RR Lyrae stars. Table 1 contains some information on these objects, and Figure 1 shows their light curves (full and phase-folded) and associated GLS periodograms. The light curves are published online.[2] The periods are consistent with RR Lyrae variability, and the light curve shapes—in particular the possible notches just before maximum brightness for the two stars—are similar to RR1. The amplitudes, however, are much smaller than any known RR1, which have amplitudes of ∼200–350 mmag. The variability search for mmRR 1 detects only this sinusoid variability and its harmonics and aliases, while mmRR 2 shows low-amplitude variability at a number of longer periods as well. The positions of these stars in the color–magnitude diagram (CMD) are shown in Figure 2. Star mmRR 1 is blueward of the locus of RR Lyrae stars, and mmRR 2 is redward. Several of the other stars redward of the full-amplitude RR Lyrae variables show low-amplitude variability at multiple periods in the approximate range 0.3–5 days.

We note a possible third star of interest, *Gaia* DR2 6045489283174903168 (G3168), which has a ∼0.64 day sinusoidal period and ∼0.5 mmag amplitude and is in the locus of RR Lyrae variables (marked in Figure 2 with a black cross). We do not include it as an mmRR because it has stronger variability than mmRR 2 at other periods (for example, a sinusoid variability at 1.67 day period of slightly smaller amplitude than the 0.64 day signal). We will further discuss this and the other M4 variables in a future work.

2.3. Blend Scenarios

Figure 3 shows images of the two mmRRs, with nearby *Gaia* DR2 sources marked. The aperture used for photometry extraction is indicated, which has a radius of 2.25 *Kepler* pixels, or ∼9″. Both the apertures used and the individual *K*2 pixels that these stars lie on are significantly blended. We focused our blend analysis on mmRR 1 due to its higher signal-to-noise ratio (S/N), but many of our conclusions extend to mmRR 2.

We searched for variability among the blended sources by using an array of 0.51 pixel radius apertures on and around mmRR 1 to obtain focused photometry of the blended objects from the *K*2 data. This photometry underwent the same roll decorrelation previously described, but not TFA cleaning. We then searched for variability at a period and flux amplitude matching the aperture centered on mmRR 1. Three apertures had a corresponding variability: the one centered on mmRR 1, and the two apertures located 0.51 pixels left and right roughly along the *x*-axis of the image in Figure 3. We concluded the variability source could only be mmRR 1, *Gaia* DR2 6045466571377393792 (Blend 1, marked in Figure 2 with a red x), or an unresolved blended source.

Blend 1's location (the blue cross in Figure 2) in the CMD is unusual, particularly given its >99% probability of cluster membership. The *Gaia* detector windows to measure G_{BP} and G_{RP} are 2.″1 × 3.″5 (Arenou et al. 2018), so it is possible that the color measurements are significantly blended with mmRR 1, perhaps inhomogeneously between the two filters for it to appear bluer than mmRR 1. It is also possible that Blend 1 is a subdwarf B (sdB) star or a white dwarf (WD) blended with a main sequence (MS) star. We were unable to determine any physical MS–WD combination that matched the measured color and magnitude for this object. Many sdB stars are variable, but none in a way that matches the variability seen for

[2] https://doi.org/10.5281/zenodo.2220532, Wallace et al. (2018).

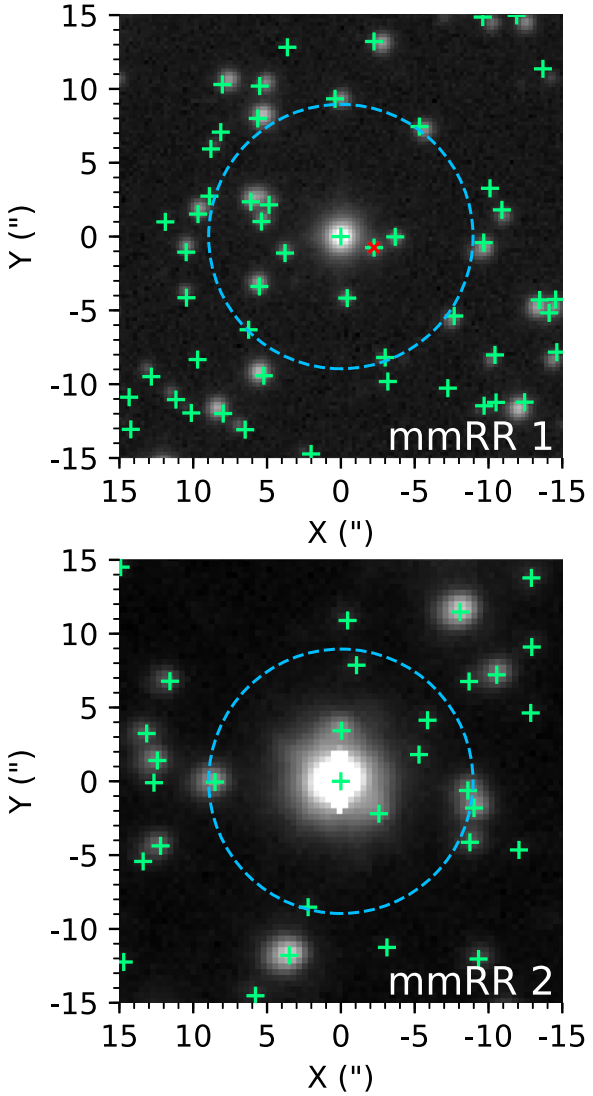

Figure 3. Images of the two variable stars. Crosses mark *Gaia* DR2 source positions. Blend 1 is additionally marked with a red x. The blue circles mark the size of aperture used for photometry extraction from the *K*2 data. The image for mmRR 1 is from the M4 reference image of Kaluzny et al. (2013) and is rotated slightly relative to the *Gaia* source positions. The image for mmRR 2 (saturated in this image) was taken with a Sinistro detector on an LCOGT 1-m telescope operated by Las Cumbres Observatory. The pixels in all three images are expressed in a logarithmic scale.

this object (which, given the $G \approx 18$ mag of this object, would need to have a ∼0.1 mag amplitude). All known types of sdB variables are some combination of too short of period, too small of amplitude, or too incoherent of pulsations to explain the variability (Catelan & Smith 2015, chapter 12). We also were unable to find any ellipsoidal variability of an sdB–MS binary that provided the necessary variability amplitude (the highest unblended amplitudes obtained were ∼0.01 mag).

If the color measurements are in error and this is an MS star, the only variability scenarios that could match the observed shape and period are the rapid rotation of a heavily spotted star or an ellipsoidal variability. We were unable to find any physically plausible ellipsoidal variability scenarios that matched the observed variability and *G*-band magnitude. To estimate the probability of blending with a heavily spotted fast rotator, we looked through the light curves for all objects with $G > 15$ and found five objects with periods that are less than one day and sinusoidal variability of roughly appropriate amplitude when blended with an HB object. The search field was ∼149 square arcminutes. From the aperture analysis we know the blend must be within about a *Kepler* pixel radius (∼4″), so the probability of one of these objects blending with mmRR 1 is $\sim 5 \times 10^{-4}$. The probability of finding two chance alignments out of 24 targets is very small at $\sim 7 \times 10^{-5}$.

Returning to mmRR 1, the orbital separation needed for a ∼0.66 day binary orbit including mmRR 1 is ∼3–4 $R_\odot$. *Gaia* DR2 (Andrae et al. 2018) measures the radius of mmRR 1 to be 2.8–4.1 $R_\odot$ (16th–84th percentiles). We used PHOEBE (Prša & Zwitter 2005) to examine contact binary scenarios and could find no physical scenario with the radius of mmRR 1 being larger than ∼2.4 $R_\odot$, the Roche limit. If the radius of mmRR 1 is indeed exceptionally small to allow a contact binary scenario, only companions with masses between 0.08 $M_\odot$ (with a face-on orbit) and ∼1 Jupiter mass (with inclination $\lesssim$45°) could produce millimagnitude amplitudes. Given the even larger radius that mmRR 1 would have had when on the red giant branch, such a system would be a post-common-envelope binary. Approximately one-third of WDs are known to have short-period post-common-envelope binary companions, with the majority having secondary stars of mass less than 0.25 $M_\odot$ (Schreiber et al. 2010). While we are unaware of estimates for the occurrence rate of such systems with HB primary stars, the possibility of an HB star having a low-mass contact binary companion cannot be dismissed out of hand. However, finding two of these systems on low-inclination orbits (which are less likely than higher inclinations assuming random orientations), without also finding systems on higher-inclination (and thus higher photometric amplitude) orbits, is unlikely. Moreover, the inconsistency between the measured stellar radius from *Gaia* and the upper limit on the radius for a contact binary is strong evidence that this scenario does not explain the observations.

Finally, we consider an undetected background RR1 or short-period Cepheid variable. An RR1 would need to be ∼200–350 times dimmer than mmRR 1 to get a millimagnitude blended amplitude. With mmRR 1 having $G = 13.23$, the background RR1 would need to have $G \approx 18.9$–19.6. We used the *Gaia* DR2 RR Lyrae variable catalog (Clementini et al. 2018; Holl et al. 2018) to determine the surface density of RR Lyrae variables with *G* magnitudes in the appropriate range in the field near M4, finding ∼2 RR Lyrae variables per 0.7 square degrees. Mirroring our estimation of rapidly rotating spotted star blending, we get a blend probability of $\sim 6 \times 10^{-6}$. The probability of finding 2 chance alignments out of 24 targets is vanishingly small at $\sim 1 \times 10^{-8}$. Even if the catalog of RR Lyrae that we are using has a completeness as low as 15%, as it does in the Galactic Bulge (Holl et al. 2018, Table 3), the probability of chance alignment is still minuscule. There are even fewer background Cepheid variables (*Gaia* detected none in the areas where we searched for RR Lyrae variables) and they typically have much longer periods, so the probability of blending with a background Cepheid is even smaller.

The S/N for mmRR 2 was not high enough for our small aperture array to disentangle specific possible sources of the variability. We note, however, that all of the *Gaia* DR2 sources within 5″ of mmRR 2 are proper motion members of the cluster . Because of this, arguments similar to those for the possible blend scenarios of mmRR 1 and Blend 1 prevail. We note that mmRR 2 has a relatively large radius in *Gaia* DR2

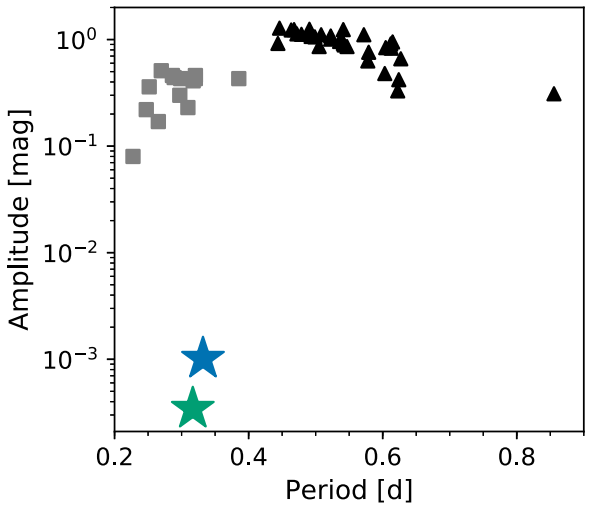

Figure 4. Periods and amplitudes of the two mmRRs and the RR Lyrae stars in M4. As in Figure 2, the blue star marks mmRR 1, and the green star marks mmRR 2. RR0 are shown as black triangles and RR1 are shown as gray squares. The data for RR Lyrae variables are from Clement et al. (2001). The two new variables have much lower amplitudes than any RR Lyrae star in the cluster.

(7.8–8.3 $R_\odot$), which would make it impossible to host a binary object at a ∼0.63 day period orbit. We also checked that the periods of the three variables do not match any previously identified RR Lyrae star in the cluster, nor do they match any other variable signal found in our light curves from the M4 superstamp. *Gaia* detects no variables within 10″ of the two mmRRs.

3. Discussion

From the evidence presented, we conclude that the most likely explanation for the observed variability is a previously unreported kind of stellar variability that, based on the locations in the CMD and variability periods and shapes, is possibly related to RR Lyrae variability. Figure 4 shows the periods and amplitudes of the mmRRs relative to the RR Lyrae variables in M4. Their amplitudes (mmRR 1:1.0 mmag, mmRR 2:0.3 mmag) are much lower than any previously observed RR Lyrae star, which have amplitudes of ∼200 mmag and greater.

We note here Buchler et al. (2005, 2009), who used data from the MACHO and OGLE databases to find ∼30 objects near the Cepheid instability strip of the Large Magellanic Cloud (LMC) with amplitudes $\lesssim$0.01 mag. At least ∼20 of these objects are members of the LMC. These match the predicted strange Cepheids of Buchler et al. (1997). These mmRRs may be the very similar strange RR Lyrae predicted by Buchler & Kolláth (2001). The amplitudes, shapes, and CMD locations match the predictions, but the periods (which would be coming from the eighth to tenth radial overtones) are longer than predicted.

We also note once again G3168, the possible third mmRR we found, as well as the other HB stars redward of the known RR Lyrae stars that had multi-periodic photometric variability of periods of approximately 0.3–5 days. These stars are perhaps connected to the mmRRs and will be described more completely later.

If these objects do represent a new class of variability, why have no similar objects been discovered previously? As mentioned in Section 1, *Kepler*/*K*2 has enabled the discovery of very small-amplitude modes in RR Lyrae variables, seemingly commonplace yet undetected in over a century of observations of these stars. The mmRRs appear to share a similar story. We make particular mention of RR Lyr, an RR0, which has been shown by *Kepler* to have small-amplitude first-overtone pulsations (Molnár et al. 2012), a phenomenon perhaps connected to these mmRRs. Finally, theoretical work indicates that convection and viscous damping are the likely physical process that set the amplitudes of RR Lyrae variables (Kolláth et al. 1998; Smolec & Moskalik 2008; Geroux & Deupree 2013); mmRRs could be valuable in further developing this understanding.

We thank A. Vanderburg for assistance with the roll decorrelation and W. Pych for providing CASE light curves that were useful in our initial vetting. G.Á.B. thanks J. Jurcsik, G. Kovács, and L. Molnár for useful discussions while at Konkoly Observatory. This research includes data collected by the *K*2 mission, funding for which is provided by the NASA Science Mission directorate. The *K*2 data were obtained from the Mikulski Archive for Space Telescopes (MAST). STScI is operated by the Association of Universities for Research in Astronomy, Inc., under NASA contract NAS5-26555. Support for MAST for non-*Hubble Space Telescope* data is provided by the NASA Office of Space Science via grant NAG5-7584 and by other grants and contracts. This research includes data from the European Space Agency (ESA) mission *Gaia* (https://www.cosmos.esa.int/gaia), processed by the *Gaia* Data Processing and Analysis Consortium (DPAC, https://www.cosmos.esa.int/web/gaia/dpac/consortium). Funding for the DPAC has been provided by national institutions, in particular the institutions participating in the *Gaia* Multilateral Agreement. This research has made use of the SIMBAD database (operated at CDS, Strasbourg, France), NASA's Astrophysics Data System Bibliographic Services, and observations from the LCOGT network.

Facilities: du Pont (TEK5 2K), *Gaia*, *Kepler*, LCOGT (Sinistro).

Software: `astrobase` (Bhatti et al. 2017), `astropy` (Astropy Collaboration et al. 2018), `FITSH` (Pál 2012), `k2mosaic` (Barentsen 2016), `matplotlib` (Hunter 2007), `numpy` (Oliphant 2006), `PHOEBE 1.0` (Prša & Zwitter 2005), `scikit-learn` (Pedregosa et al. 2011), `scipy` (Jones et al. 2001), `VARTOOLS` (Hartman & Bakos 2016).

ORCID iDs

Joshua J. Wallace https://orcid.org/0000-0001-6135-3086
Joel D. Hartman https://orcid.org/0000-0001-8732-6166
Gáspár Á. Bakos https://orcid.org/0000-0001-7204-6727
Waqas Bhatti https://orcid.org/0000-0002-0628-0088

References

Andrae, R., Fouesneau, M., Creevey, O., et al. 2018, A&A, 616, A8
Arenou, F., Luri, X., Babusiaux, C., et al. 2018, A&A, 616, A17
Astropy Collaboration, Price-Whelan, A. M., Sipőcz, B. M., et al. 2018, AJ, 156, 123
Baglin, A. & & COROT Team 1998, in IAU Symp. 185, New Eyes to See Inside the Sun and Stars, ed. F.-L. Deubner, J. Christensen-Dalsgaard, & D. Kurtz (Cambridge: Cambridge Univ. Press), 301
Barentsen, G. 2016, barentsen/k2mosaic: v2.0.0, Zenodo, doi:10.5281/zenodo.167343
Benkő, J. M., Kolenberg, K., Szabó, R., et al. 2010, MNRAS, 409, 1585

Bhatti, W., Bouma, L. G., & Wallace, J. 2017, astrobase, Zenodo, doi:10.5281/zenodo.1011188
Buchler, J. R., & Kolláth, Z. 2001, ApJ, 555, 961
Buchler, J. R., Wood, P. R., Keller, S., & Soszyński, I. 2005, ApJ, 631, L151
Buchler, J. R., Wood, P. R., & Soszyński, I. 2009, ApJ, 698, 944
Buchler, J. R., Yecko, P. A., & Kollath, Z. 1997, A&A, 326, 669
Catelan, M., & Smith, H. A. 2015, Pulsating Stars (New York: Wiley)
Clement, C. M., Muzzin, A., Dufton, Q., et al. 2001, AJ, 122, 2587
Clementini, G., Ripepi, V., Molinaro, R., et al. 2018, arXiv:1805.02079
Gaia Collaboration, Brown, A. G. A., Vallenari, A., et al. 2016a, A&A, 595, A2
Gaia Collaboration, Prusti, T., de Bruijne, J. H. J., et al. 2016b, A&A, 595, A1
Geroux, C. M., & Deupree, R. G. 2013, ApJ, 771, 113
Hartman, J. D., & Bakos, G. Á 2016, A&C, 17, 1
Holl, B., Audard, M., Nienartowicz, K., et al. 2018, A&A, 618, A30
Howell, S. B., Sobeck, C., Haas, M., et al. 2014, PASP, 126, 398
Hunter, J. D. 2007, CSE, 9, 90
Jones, E., Oliphant, T., Peterson, P., et al. 2001, SciPy: Open source scientific tools for Python, http://www.scipy.org/
Kaluzny, J., Thompson, I. B., Rozyczka, M., & Krzeminski, W. 2013, AcA, 63, 181
Kolláth, Z., Beaulieu, J. P., Buchler, J. R., & Yecko, P. 1998, ApJ, 502, L55
Kovács, G., Bakos, G., & Noyes, R. W. 2005, MNRAS, 356, 557
Kovács, G., Zucker, S., & Mazeh, T. 2002, A&A, 391, 369
Lindegren, L., Hernández, J., Bombrun, A., et al. 2018, A&A, 616, A2
Lindegren, L., Lammers, U., Bastian, U., et al. 2016, A&A, 595, A4
Lomb, N. R. 1976, Ap&SS, 39, 447
McQuillan, A., Aigrain, S., & Mazeh, T. 2013, MNRAS, 432, 1203
Molnár, L. 2018, in Proc. Polish Astronomical Society 6, Revival of the Classical Pulsators: from Galactic Structure to Stellar Interior Diagnostics, ed. R. Smolec et al. (Warsaw: Polskie Towarzystwo Astronomiczne), 106
Molnár, L., Kolláth, Z., Szabó, R., et al. 2012, ApJ, 757, L13
Oliphant, T. 2006, Guide to NumPy (Trelgol Publishing) http://www.tramy.us/numpybook.pdf
Pál, A. 2012, MNRAS, 421, 1825
Pedregosa, F., Varoquaux, G., Gramfort, A., et al. 2011, Journal of Machine Learning Research, 12, 2825 (http://www.jmlr.org/papers/v12/pedregosa11a.html)
Prša, A., & Zwitter, T. 2005, ApJ, 628, 426
Riello, M., De Angeli, F., Evans, D. W., et al. 2018, A&A, 616, A3
Scargle, J. D. 1982, ApJ, 263, 835
Schreiber, M. R., Gänsicke, B. T., Rebassa-Mansergas, A., et al. 2010, A&A, 513, L7
Smolec, R., & Moskalik, P. 2008, AcA, 58, 193
Soares-Furtado, M., Hartman, J. D., Bakos, G. Á., et al. 2017, PASP, 129, 044501
Stellingwerf, R. F. 1978, ApJ, 224, 953
Vanderburg, A., & Johnson, J. A. 2014, PASP, 126, 948
Vanderburg, A., Latham, D. W., Buchhave, L. A., et al. 2016, ApJS, 222, 14
van Leeuwen, F., Evans, D. W., De Angeli, F., et al. 2017, A&A, 599, A32
Walker, G., Matthews, J., Kuschnig, R., et al. 2003, PASP, 115, 1023
Wallace, J., Hartman, J., Bakos, G., & Bhatti, W. 2018, Light curves for M4 millimagnitude RR Lyrae (mmRR), Zenodo, doi:10.5281/zenodo.2220532
Wallace, J. J. 2018, RNAAS, 2, 213
Zechmeister, M., & Kürster, M. 2009, A&A, 496, 577